ORIGINAL PAPER

Hydrophobic interaction-mediated reversible adsorption–desorption of nanoparticles in the honeycomb-patterned thermoresponsive poly(*N*-isopropylamide) hydrogel surface

Jin Kyung Kim · Kyu Ho Jung · Ji Ho Jang · Do Sung Huh

Abstract Hydrophobic interaction-mediated reversible adsorption–desorption of Ag nanoparticles in water solutions was studied in surface-tailored poly(*N*-isopropylacrylamide) (PNIPAAm) hydrogel film. Surface-tailoring of PNIPAAm hydrogel was performed by the preparation of the hydrogel as a honeycomb-patterned film using a honeycomb-patterned PS film as a template. The surface morphology and hydrophobic interaction of the patterned hydrogel surface were significantly altered by temperature change of the aqueous solution that came in contact with the gel. The surface of the hydrogel became hydrophobic for adsorption at a higher temperature than the lower critical solution temperature of 32 °C, but became hydrophilic with decreased adsorptivity at lower temperature condition. Adsorptivity was obtained through measuring the concentration of the silver nanoparticles using UV–vis spectroscopy in an aqueous solution. A reversible adsorption–desorption of nanoparticles dependent on the temperature in the hydrogel surface obtained in this study clearly suggested that the hydrophobic interaction was reversibly changed in the patterned temperature-responsive hydrogel surface, similar to various biological systems in nature.

Keywords Thermoresponsive hydrogel surface · Hydrophobic interaction · Adsorption–desorption · Nanoparticles · Honeycomb-pattern

Introduction

Many polymer scientists have recently focused on smart hydrogels that can undergo reversible, three-dimensional, large-scale physical or chemical changes in response

J. K. Kim · K. H. Jung · J. H. Jang · D. S. Huh (✉)
Department of Chemistry and Nano Science and Engineering, Institute of Basic Science,
Inje University, Obang 607, Gimhae, Kyungnam 621-749, South Korea
e-mail: chemhds@inje.ac.kr

to small external changes in environmental conditions, such as temperature [1], pH [2, 3], light [4], magnetic or electric field [5], ionic strength [6], and biological molecules [7].

The hydrogel response mechanism is based on the chemical structure of the polymer network. Among stimuli-responsive hydrogels, temperature-responsive hydrogels are the most studied because of their potential applications in the biomedical field, such as in therapeutic agent delivery systems, tissue engineering scaffolds, cell culture supports, bioseparation devices, sensors, and actuator systems [8–11].

Temperature-responsive hydrogels are usually based on polymers that exhibit lower critical solution temperature (LCST); that is, gels collapse as temperature increases. Below the LCST, hydrogen bonding between hydrophilic segments of the polymer chain and water molecules dominates, leading to enhanced dissolution in water. As the temperature increases, however, hydrophobic interactions become strengthened, while hydrogen bonding becomes weaker. The net result is shrinking of the hydrogels due to inter-polymer chain association through hydrophobic interactions. Poly(*N*-isopropylacrylamide) (PNIPAAm) and NIPAAm copolymers are the most studied among such systems [12, 13].

Despite great interests on stimuli-responsive polymers or hydrogels because of their useful and advanced functions such as drug or gene carriers with triggered release properties, the novel functions of responsive polymeric systems have an important role in detection and sensing applications. However, stimuli-responsive polymer-based detection systems are still in their infancy stage compared with the relatively mature field of small molecule probes [14, 15]. One major limitation of bulk hydrogel with regard to potential applications of stimuli-sensitive hydrogels in detection and sensing systems is the diffusion rate-limited transduction of signals. However, this limitation can be prevented by engineering interconnected pores in the polymer structure to form capillary networks in the matrix and by downscaling the size of hydrogels to significantly decrease diffusion paths [16]. More effective applications of such hydrogels require fast response to external stimuli. To attain such a response, bulk stimuli-sensitive hydrogel is reduced to smaller particles because the response rate is inversely proportional to the square of the characteristic dimension of the hydrogel [17]. As a result, the preparation of nano- or micro-sized hydrogel particles [18, 19] and the fabrication of stimuli-responsive hydrogels have become significantly important for potential applications of such materials [3, 20].

One example is the microfabrication of hydrogel on a patterned hydrogel film that can rapidly respond to external stimuli for the adsorption or desorption of nanoparticles in the hydrogel. This process is achieved by increasing the surface area of the hydrogel film, which can significantly change pattern structures in the hydrogel film for increased sensitivity to environmental conditions. A hydrogel film can be fabricated using highly ordered honeycomb-patterned porous films as templates in a method introduced by Pitois et al. [21]. Highly ordered polymer films were produced by evaporating a polymer solution in a volatile solvent under humid conditions. Water vapor condensed on the cooling surface because of rapid solvent evaporation, and the droplets were trapped on the surface of the solution via surface tension. To help the trapping of water droplets in the hydrophobic solution surface, an amphiphilic copolymer is generally used in the polymer solution, because the

polymer forms a stable monolayer at the air–water interface. Maruyama et al. [22] synthesized several kinds of neutral or ionic amphiphilic copolymers.

The simple fabrication method of honeycomb-patterned hydrogel or microlens arrays using the self-organized honeycomb-patterned films as templates was developed by H. Yabu et al. They demonstrated a novel fabrication method of micro-patterns onto thermally and chemically weak stretched polymer films using cross-linked polymer molds [the contact etching lithography (CEL) process]. The swollen mold softens only the surface of stretched polymer film, and surface patterns were easily transferred onto the stretched polymer film without any damage. After thermal shrinkage, the surface pattern was miniaturized. Further-more, when the processes were performed repeatedly, the surface patterns miniaturized further. The processes can be a good candidate for micro-patterning without using any expensive instruments and multiple processes [23].

An ordered pattern of hydrogel microspheres was also studied by Tsuji and Kawaguchi [24]. Recently, Maeda and Yoshida [25] reported the fabrication of highly ordered honeycomb surface and inverse opal structure in the PNIPAAm hydrogel via the microfabrication method using closely packed silica beads as a template. The gels can reversibly change the shapes and sizes of the pores by swelling and deswelling with temperature changes. Such a thermoregulation of surface topography can be useful for the design of functional surfaces with tunable physical properties.

Hydrophobic interaction has a prominent role in biological processes, such as in lipid bilayer formation [26], protein folding [27], and protein–protein recognition [28]. As one of the universal weak interactions in nature, hydrophobic interaction can be observed in smart hydrogel surfaces. Therefore, novel smart surfaces can be designed using weak hydrophobic interactions to reversibly adsorb and desorb target particles.

In this study, honeycomb-patterned thermosensitive PNIPAAm hydrogel films were fabricated via a facile method using photopolymerization of the pregel solution in a highly ordered polystyrene (PS) template film to change the hydrophobic interaction of the hydrogel surface depending on temperature, which induces the change of adsorptivity of the hydrogel surface to nanoparticles existing in aqueous solution. The reversible change in the surface morphology of the hydrogel film dependent on temperature was measured by scanning electron microscopy (SEM). For the reversible adsorption–desorption of nanoparticles on the hydrogel surface based on the dynamic pattern change of the hydrogel surface in response to temperature, the concentration of silver nanoparticles in an aqueous solution was measured via flowing ultraviolet–visible spectrometry (UV–vis).

Experimental

Materials

A PS standard (average MW 400,000 g mol^{-1}, Aldrich Co. product no. 330353) was used for the synthesis of the honeycomb-patterned PS template film. Tetrathiafulvalene (TTF) was purchased from John Mattey Co. Silver nitrate

(AgNO$_3$), poly(*N*-vinylpyrrolidone) (PVP, average MW 40,000 g mol^{-1}), *N,N'*-methylenebisacrylamide (MBAA), 2,2-dimethoxy-1,2-diphenylethan-1-one (Irgacure 651), chloroform (99.8 %), acetonitrile (99.8 %), and ethanol (99.8 %) were all obtained from Aldrich Co. *N*-Isopropylacrylamide (NIPAAm) was purchased from Tokyo Chemical Industry.

Preparation of honeycomb-patterned PNIPAAm hydrogel film

Fabricating the honeycomb-patterned, temperature-responsive hydrogel film was carried out via photopolymerization of *N*-isopropylacrylamide (NIPAAm) on the patterned PS template films. The detailed procedure for the preparation of the honeycomb-patterned PS thin film was presented in our previous report [29]. A solution of PS in chloroform was cast on a petri dish and allowed to completely evaporate under humid conditions, thus obtaining an opaque film. Highly ordered honeycomb-patterned PS films were obtained by adding an amphiphilic copolymer (P$_{am}$) to the PS solution. The copolymer was prepared via copolymerization of *N*-dodecylacrylamide and 6-hexaamido acrylic acid [23].

For the photopolymerization of NIPAAm on the patterned PS template films, NIPAAm (11.32 g, 4.0 M), MBAAm (0.125 g, 0.08 M), and Irgacure 651 (0.256 g, 0.1 M) were dissolved in ethanol as a pregel solution. Photopolymerization was performed in a self-manufactured vacuum chamber. The PS template on the petri dish was placed in a vacuum chamber, and 4 mL of pregel solution was poured on the petri dish to fabricate a convex-patterned hydrogel film. After removing the air from the vacuum chamber using a vacuum pump for 1 min, the chamber was filled with nitrogen. The mold was then exposed to UV light (Hamamatsu Co. L8252A) for 5 min on the template. The patterned PNIPAAm hydrogel film was prepared by peeling the hydrogel film from the PS template, and then rinsing it with deionized water. The complete scheme for the preparation of the honeycomb-patterned PNIPAAm hydrogel film is illustrated in Fig. 1a.

Dynamic pattern change of the hydrogel surface in response to temperature

Patterned PNIPAAm hydrogel films were soaked in distilled water at 27, 32, and 37 °C by considering the phase-transition temperature (LCST) of the PNIPAAm hydrogel (ca. 32 °C). The convex-patterned gel films that equilibrated at a given temperature were observed at first by optical microscopy (Olympus BX51) and observed in more detail via SEM (COXEM CX-100s). Before observation by SEM, the gels were quickly frozen by soaking them in liquid nitrogen and lyophilized for 24 h. In addition to the change of surface morphology of the patterned hydrogel in response to temperature, the reversibility of the surface morphology of hydrogel film was also checked by repeated soaking of the hydrogel at 27 and 37 °C water.

Temperature-responsive Ag adsorption on the PNIPAAm hydrogel surface

Experiments for the temperature-responsive Ag adsorption were performed in the aqueous solution containing Ag nanoparticles at 27 and 37 °C to compare the
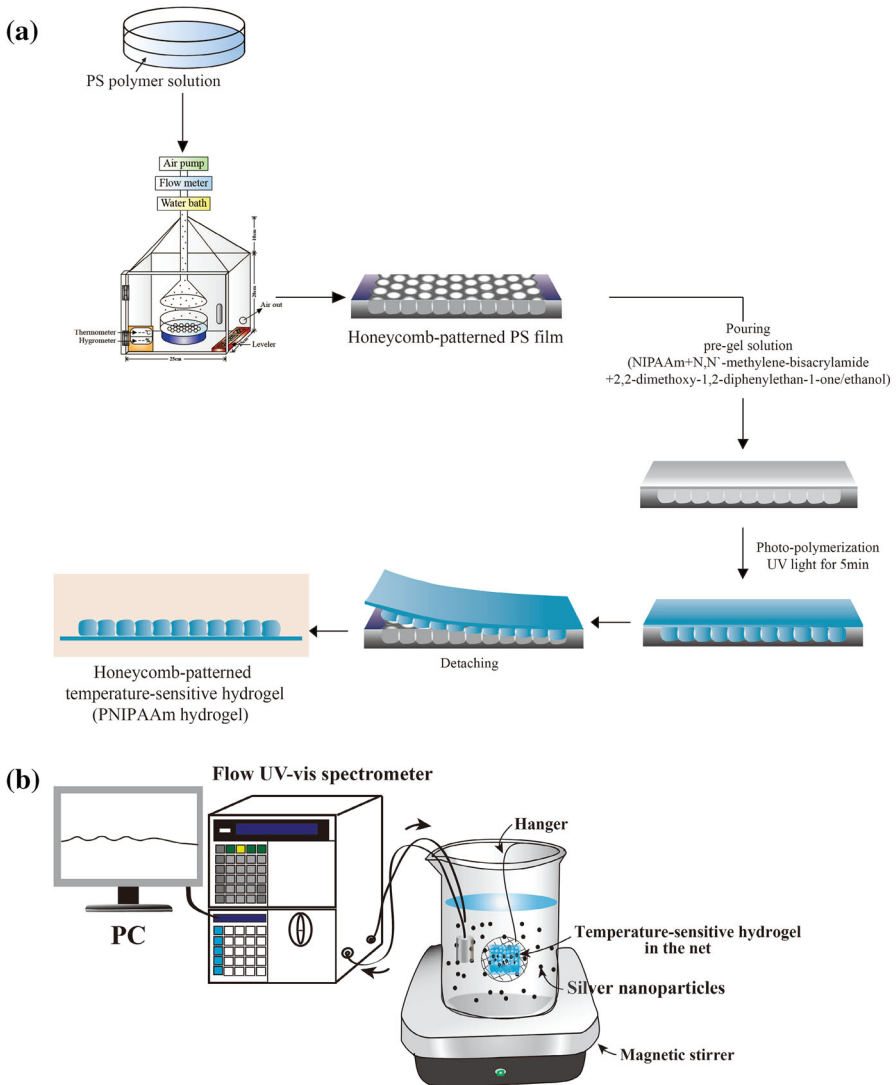
Fig. 1 a Overall experimental scheme for the preparation of the honeycomb-patterned PNIPAAm hydrogel film using a honeycomb-patterned polystyrene film as a template. **b** The experimental scheme for the measurement of Ag adsorption to patterned hydrogel surface in real time

adsorptivity below and above LCST in the PNIPAAm hydrogel surface. This process was achieved by measuring change in Ag concentration in the water solution under stirred condition. For the measurement, the patterned hydrogel film cut into 1.0 cm × 1.0 cm × 1.0 mm dimensions was placed into a net, and then hanged in 0.01 M silver solution with 25 mL water. The Ag adsorption to patterned hydrogel surface was detected with a flowing UV–vis detector (Hitachi L-7400) at a constant flow rate of 2.0 mL/min with constant wavelength of 450 nm. Ag

nanoparticles were prepared by reducing AgNO$_3$ using TTF and PVP, respectively. TTF derivatives act as electron donors, and then form stable charge-transfer complexes with various organic and inorganic acceptor species [30]. The procedure for Ag metallization was introduced in our previous report [31]. AgNO$_3$ was dissolved in 25 mL acetonitrile, and a small amount of PVP was added to the solution to inhibit the aggregation of the reduced Ag particles. TTF was then added to the solution under vigorous stirring at room temperature, and the PS template film was soaked in the solution to adhere the reduced Ag nanoparticles onto the film surface for 24 h. The color of the reaction mixture gradually changed from yellow to dark brown under continuous stirring. The Ag nanoparticle-coated PS template film was drawn from the beaker and cleaned by water several times to remove the unreduced silver ions and other reactants. After then, pure Ag solution was prepared by soaking the Ag nanoparticle-coated PS template film to a new beaker containing pure water. Ag nanoparticles were separated from the PS template film by stirring in the aqueous solution and finally the PS template was also removed from the solution. The experimental scheme for the measurement of Ag adsorption to patterned hydrogel surface is illustrated in Fig. 1b.

Results and discussion

Preparation of honeycomb-patterned hydrogel surface

Figure 2a shows the typical SEM image for the honeycomb-patterned PAA hydrogel film. A surface image is shown on the left and a cross-sectional image is shown on the right. Fabricating the honeycomb-patterned PNIPAAm hydrogel film was carried out via photopolymerization of NIPAAm using MBAAm as cross-linker and honeycomb-patterned PS film as a template. Figure 2b shows the SEM image of the honeycomb-patterned PS film used for the template obtained by evaporating the PS solution under humid conditions. The patterned PAA hydrogel film exhibited convex and hexagonal structures with regular order, indicating that the experimental method in this study, that is, using the template PS film, was an effective and facile method for preparing a micro-patterned hydrogel film. Direct formation of hydrogels with honeycomb-patterned structures via evaporation of polymer solutions under humid conditions is impossible because the hydrogel polymer solution is not hydrophobic and a cross-linker should be used in gelation.

Dynamic pattern change of the patterned hydrogel surface in response to temperature

Figure 3a–c shows the structure of the patterned hydrogels after 10 min of soaking in water at 27, 32, and 37 °C, respectively obtained by the optical microscopy. Although the structure of patterns is not clear in the photo images, the structural change of the patterned hydrogel by temperature of water is vaguely discriminated between Fig. 3a–c. The magnified inset figures more clearly show the change of surface morphology of the hydrogel structure depending on the environmental
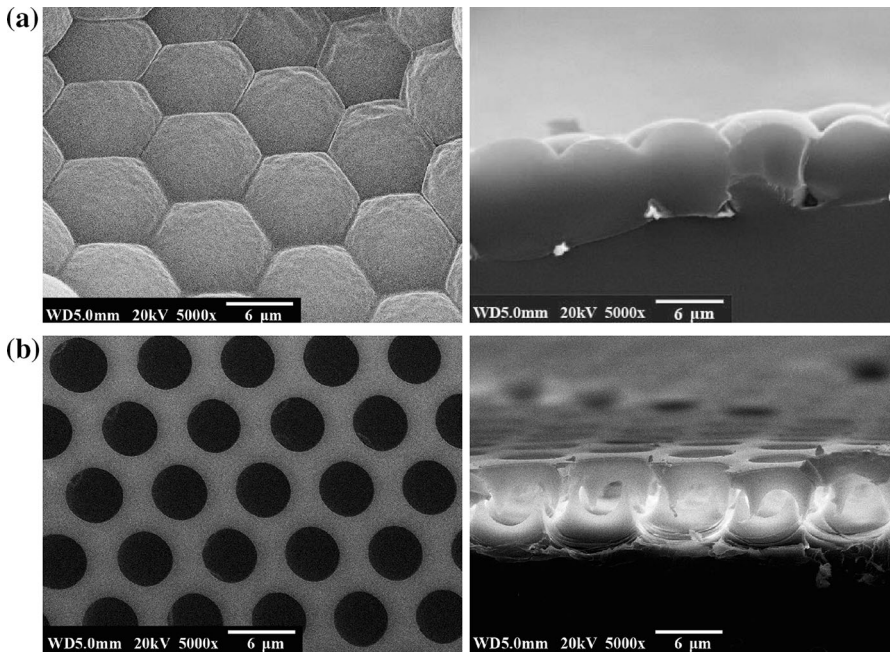
Fig. 2 **a** Typical SEM image for the honeycomb-patterned PNIPAAm hydrogel film (*left* surface image, *right* cross-sectional image). **b** The SEM image of the honeycomb-patterned PS film used for the template obtained by evaporating the PS solution under humid conditions

temperature of water. However, an obvious structural change is well shown by the SEM images given in Fig. 4a–c. The comparison of the SEM images shown in Fig. 4a–c indicates that surface morphology of the hydrogel surface is sensitive to the variations in the environmental temperature of water. The degree of swelling of the surfaces of the hydrogel film varied. The hexagonal patterns of the PNIPAAm hydrogel film after soaking below LCST at 27 °C water did not change significantly compared with the original state (Fig. 2a); however, the patterned surface became slightly swollen, as shown in Fig. 4a. Meanwhile, the patterned hydrogel, after being soaked in high-temperature water with an approximate LCST of 32 °C, exhibited a slightly squeezed state compared with the state below LCST, as shown in Fig. 4b. However, the patterned hydrogel, after being soaked in higher temperature water of 37 °C above LCST, was transformed into a greatly squeezed state, thus inducing a deformed or irregularly patterned structure, as shown in Fig. 4c. The structure seems to be more adhesive at a glance with great hydrophobic interaction.

Although the comparison of the SEM images shown in Fig. 4a–c indicates that the surface morphology of the hydrogel surface is sensitive to the environmental temperature of water, a more important result regarding temperature dependency of surface morphology should be the reversibility of surface pattern obtained by repeated change of water temperature for the same gel. The reversibility of pattern
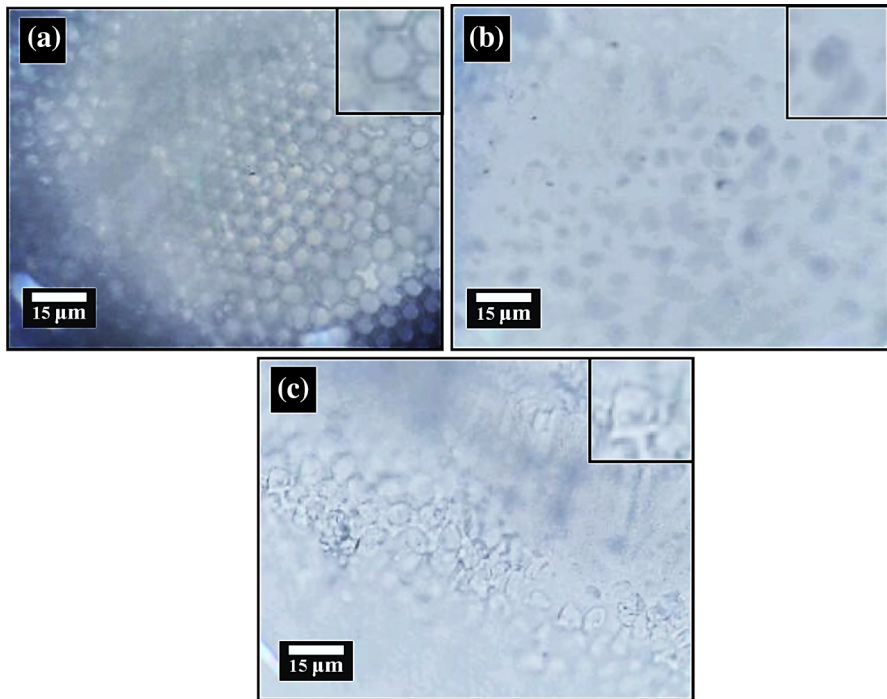
Fig. 3 The photo images obtained by the optical microscopy indicating the dependence of the surface morphology of the hydrogel surface on environmental temperature after soaking the hydrogel in water with different temperatures: **a** 27 °C, **b** 32 °C, and **c** 37 °C, respectively

morphology and hydrophobic interaction induced by the pattern change can be a key issue when considering the application of the hydrogel as a biomimetic smart material. The SEM images shown in Fig. 4d suggest the reversibility of surface morphology. Left and right images were obtained by soaking of a hydrogel alternatively at 27 and 37 °C water, respectively. Left image was obtained at 27 °C water while right image was obtained at 37 °C water in the repeated process. A similar structure was recovered with the patterns obtained by a separate temperature system although the pattern is not exactly the same as those in Fig. 4a–c. However, the fact that a deformed and high surface area pattern at 37 °C is recovered as a similar structure presented in Fig. 4c is very stimulating.

Temperature-responsive Ag adsorption on the PNIPAAm hydrogel surface

Figure 5a shows the change of absorbance in the flowing UV–vis in which the absorbance was fixed at 450 nm, corresponding to the characteristic peak of Ag nanoparticles. This absorbance change quantifies real-time concentration of Ag nanoparticles remaining in the water solution without adsorption to the hydrogel surface. The figure indicates that Ag nanoparticles in the water solution were gradually adsorbed onto the hydrogel surface with the soaking time because the
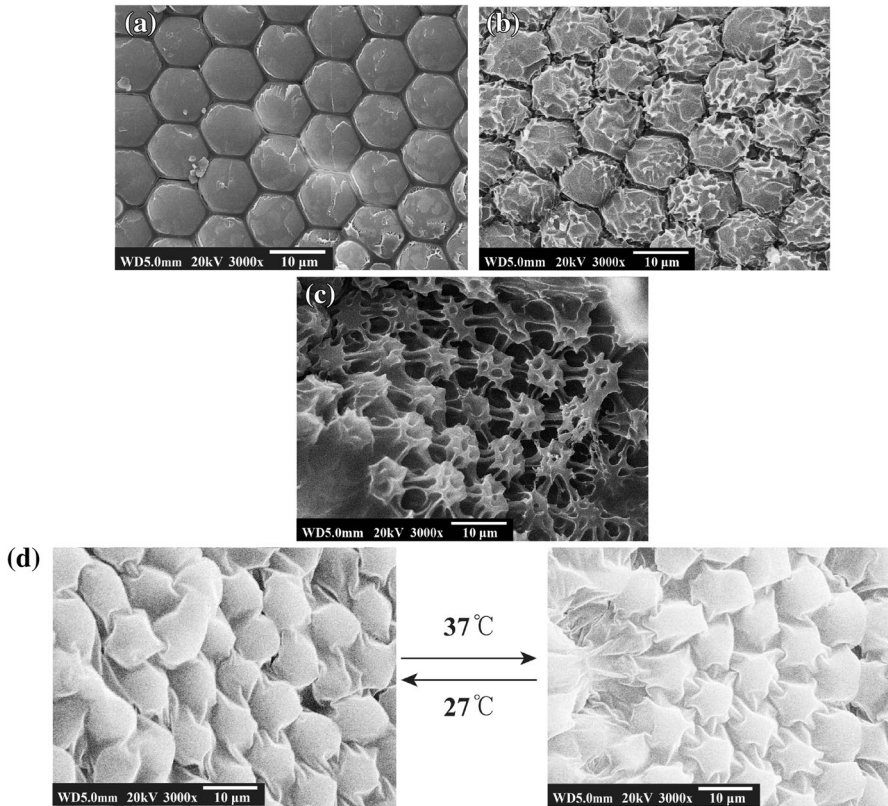
Fig. 4 The SEM images indicating the dependence of the surface morphology of the hydrogel surface on environmental temperature after soaking the hydrogel in water with different temperatures: **a** 27 °C, **b** 32 °C, and **c** 37 °C, respectively, and **d** shows the reversibility of the surface morphology by repeated soaking of the hydrogel between 27 and 37 °C water

absorbance of the solution was decreased. However, the slopes of the two curves were significantly different, indicating that adsorptivity was greatly affected by the temperature of water. The comparison of adsorptivity dependent on temperature shows that the adsorptivity of the hydrogel surface was higher at 37 °C water than at 27 °C water. This result can be attributed to two reasons. The first is due to the pattern change of the hydrogel surfaces in response to temperature change, as shown in Fig. 4a–c. The surface pattern shown in Fig. 4c obtained by a higher temperature has a more favorable structure for the adsorption of nanoparticles by a higher surface area with a porous structure. The second factor is the hydrophobic interaction of the hydrogel surface that is dependent on temperature. The surface of the temperature-responsive PNIPAAm hydrogel exhibits a hydrophobic state and, therefore, becomes very sticky at a temperature above LCST, because bound water molecules are released outside with a large gain in entropy. By contrast, water molecules form hydrogen bonds with polar groups on the polymer backbone and
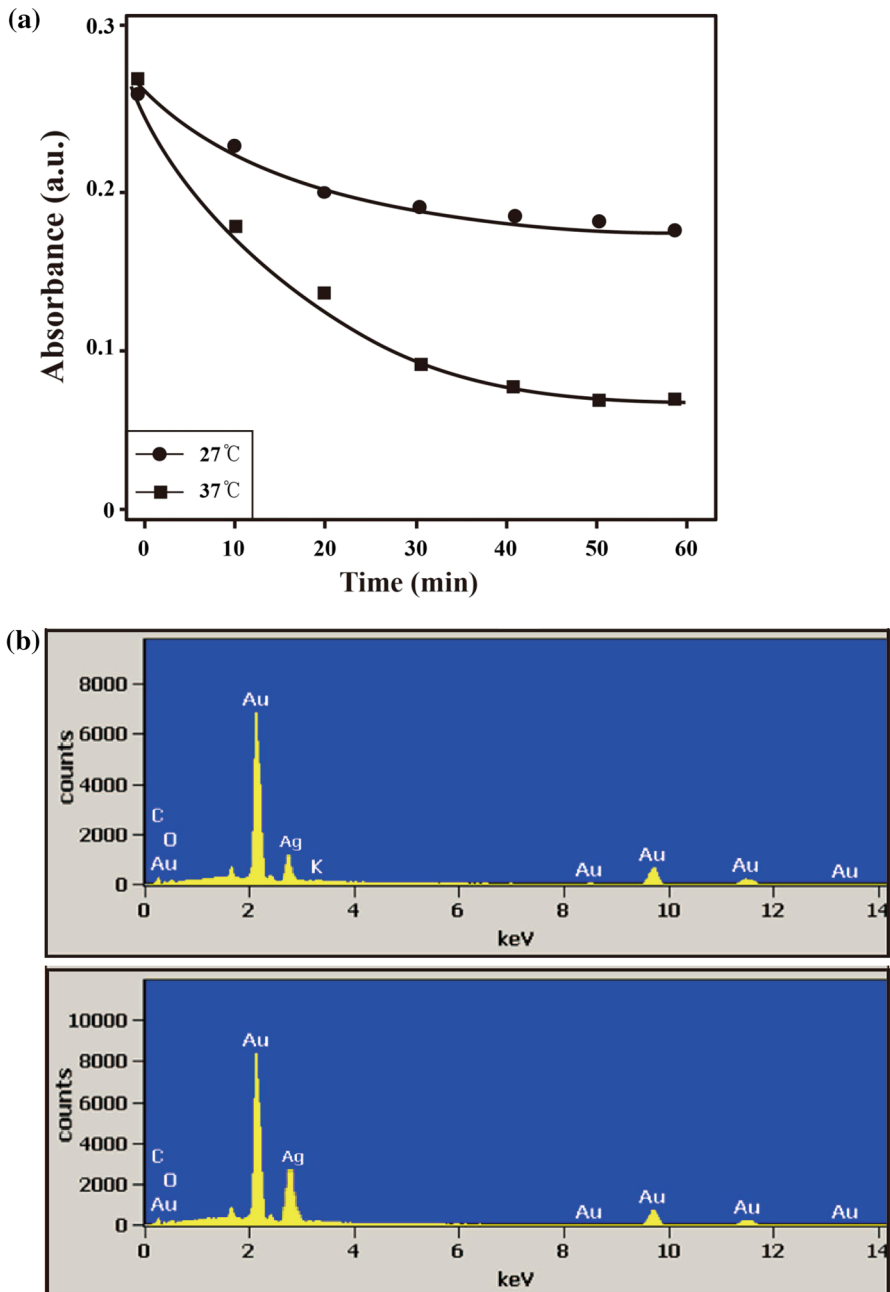
Fig. 5 Comparison of adsorptivity of the hydrogel surface to the silver nanoparticles. **a** The change of absorbance in the flowing UV–vis in which the absorbance was fixed at 450 nm for the concentration of silver nanoparticles. **b** SEM–EDS images indicating the absorptivity: *Top* image was obtained by 10 min soaking of the hydrogel into 0.01 M silver nanoparticles solution at 27 °C while *bottom* image was obtained by soaking at 37 °C solution

organize around hydrophobic groups for the hydrophilic surface with lower adsorptivity below LCST.

The SEM–EDS image of Fig. 5b shows the direct evidence of adsorptivity of nanoparticles on the patterned hydrogel surface depending on environmental temperature. Top image was obtained after soaking of a hydrogel film for 10 min in 0.01 M Ag solution at 27 °C, while bottom image was obtained by soaking at 37 °C. The peak of Ag is certainly higher in the case of 37 °C than 27 °C, which means that the adsorptivity is higher in high-temperature water. The peak of Au seems to be originated by the coated gold for the SEM image.

In spite of the difference in adsorptivity of the patterned hydrogel surface in response to temperature, as shown in Fig. 5a, b, we cannot draw a conclusion that greatly adsorbed silver nanoparticles at a higher temperature above LCST are released to the water when the temperature of water is decreased below LCST, and are re-adsorbed if the temperature is increased. Such finding indicates the reversible adsorption–desorption of nanoparticles on the hydrogel surface depending on temperature.

Reversible adsorption–desorption of silver nanoparticles on the hydrogel surface

Figure 6 shows the result of the reversible adsorption–desorption of silver nanoparticles on the hydrogel surface in response to temperature obtained by an alternative heating and cooling of the aqueous solution repeatedly. The repeated heating and cooling between 37 and 27 °C were performed by the application of two water baths kept at constant temperature of 45 and 15 °C, respectively. The beaker of water solution including silver nanoparticles and hydrogel film was firstly soaked into the 45 °C water bath to heat the solution about 37 °C. As shown in Fig. 6, the absorbance was rapidly decreasing with time, which was due to the adsorption of silver nanoparticles to the hydrogel surface at a higher temperature than LCST as shown in Fig. 5. After then, the beaker of water solution including silver nanoparticles and hydrogel film was taken out from the 45 °C water bath and was soaked to the 15 °C water bath for cooling the solution to about 27 °C. The absorbance was rather slightly increased with time as shown in the figure, which means that a part of the adsorbed silver nanoparticles to the hydrogel surface at 37 °C condition was rather released from the hydrogel surface to aqueous solution. It was due to the difference of adsorptivity of the hydrogel surface between 37 and 27 °C. The adsorbed amount at 37 °C is so higher than the amount which can be adsorbed at 27 °C water and, therefore, an excess of silver nanoparticles adsorbed at 37 °C water should be released to the solution phase at 27 °C. However, the adsorbed silver nanoparticles at 37 °C could not be completely released at 27 °C water because the hydrogel surface at 27 °C also adsorbs silver nanoparticles until the arrival of equilibrium. As a result, the change of absorbance by repeated heating and cooling was gradually decreased as shown in Fig. 6, which means that the change between adsorbed silver nanoparticles and released silver nanoparticles was gradually decreased. This might be due to the accumulation of silver nanoparticles on the hydrogel surface without complete releasing in spite of temperature decrease.
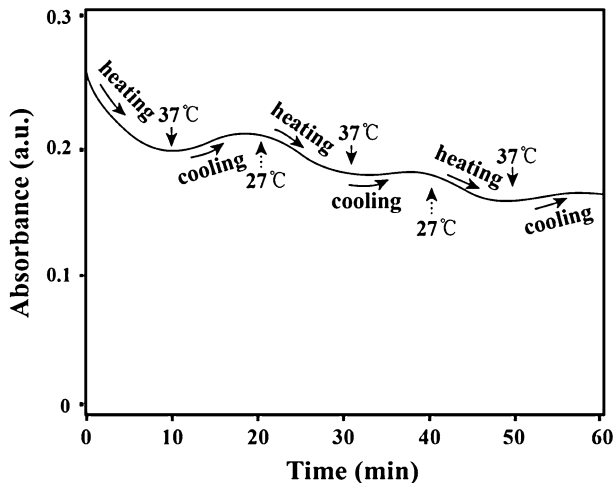
Fig. 6 The result for the reversible adsorption–desorption of silver nanoparticles on the hydrogel surface in response to temperature obtained by an alternative heating and cooling of the aqueous solution repeatedly. The repeated heating and cooling between 37 and 27 °C was performed by the application of two water baths kept at constant temperature of 45 and 15 °C, respectively

It means that the total amount of silver nanoparticles adsorbed on the hydrogel surface was gradually increased.

However, the result for the reversibility of adsorption–desorption of nanoparticles on the temperature-responsive PNIPAAm hydrogel surface obtained by an alternative heating and cooling is highly valuable because the hydrophobic interaction-mediated reversible adsorption–desorption has not been studied so much although the applications of reversible volume change of the temperature-responsive bulk PNIPAAm hydrogel have been widely studied [32]. The sensitivity of nanoparticles to the hydrogel surface can be further heightened by environmental stimuli compared with the bulk hydrogel system. As such, the major limitation of bulk hydrogel in potential applications of stimuli-sensitive hydrogels in detection and sensing systems induced by diffusion rate-limited transduction of signals can be surmounted by the patterned hydrogel surface.

Conclusion

Hydrophobic interaction-mediated reversible adsorption–desorption of Ag nanoparticles in water solutions was studied in surface-tailored PNIPAAm hydrogel. Surface-tailoring of PNIPAAm hydrogel was performed by the preparation of the hydrogel as a honeycomb-patterned film using a honeycomb-patterned PS film as a template. The surface morphology and hydropobic interaction of the patterned hydrogel surface were significantly changed by environmental temperature changes of water. The surface of the PNIPAAm hydrogel was squeezed, thus becoming sticky for adsorption at a higher temperature above the LCST of 32 °C; however,

the surface swelled and became hydrophilic with decreased adsorptivity below LCST. A reversible adsorption–desorption of nanoparticles dependent on temperature on the hydrogel surface was performed by alternative heating and cooling of the water solution using two water baths kept at 45 and 15 °C. The concentration of silver nanoparticles in water solution was changed repeatedly by temperature change, which was decreased by heating and increased by cooling. Thus, the heterogeneous reversible adsorption–desorption of nanoparticles obtained in this study clearly suggested that the hydrophobic interaction was reversibly changed in the patterned temperature-responsive hydrogel surface as a biomimetic system. Then, we can design new-type smart surfaces by utilizing hydrophobic interactions like nature reversibly capture and release target materials such as cancer cell.

References

1. Ding Z, Chen G, Hoffman AS (1998) Unusual properties of thermally sensitive oligomer-enzyme conjugates of poly(*N*-isopropylacrylamide)-trypsin. J Biomed Mater Res 9:498–505
2. Stayton PS, Shimoboji T, Long C, Chilkoti A, Chen GH, Harris JM, Hoffman AS (1995) Control of protein-ligand recognition using a stimuli-responsive polymer. Nature 378:472–474
3. Hu Z, Chen Y, Wang C, Zheng Y, Li Y (1998) Polymer gels with engineered environmentally responsive surface patterns. Nature 393:149–152
4. Hrouz J, Ilavsky M, Ulbrich K, Kopěcek J (1981) The photoelastic behaviour of dry and swollen networks of poly(*N*,*N*-diethylacrylamide) and of its copolymers with *N-tert*-butylacrylamide. Eur Polym J 17:361–366
5. Kwon IC, Bae YH, Kim SW (1991) Electrically erodible polymer gel for controlled release of drugs. Nature 354:291–293
6. Kokufuta E, Tanaka T (1991) Biochemically controlled thermal phase transition of gels. Macromolecules 24:1605–1607
7. Suzuki A, Tanaka T (1990) Phase transition in polymer gels induced by visible light. Nature 346:345–347
8. Packhaeuser CB, Schnieders J, Oster CG, Kissel T (2004) In situ forming parenteral drug delivery systems: an overview. Eur J Pharm Biopharm 58:445–455
9. Hatefi A, Amsden B (2002) Biodegradable injectable in situ forming drug delivery systems. J Control Release 80:9–28
10. Jeong B, Bae YH, Kim SW (1997) Biodegradable block copolymers as injectable drug-delivery systems. Nature 388:860–862
11. Jeong B, Gutowska A (2002) Lessons from nature: stimuli-responsive polymers and their biomedical applications. Trends Biotechnol 20:305–311
12. Hoffman AS, Affrassiabi A, Dong LC (1986) Thermally reversible hydrogels: II. Delivery and selective removal of substances from aqueous solutions. J Control Release 4:213–222
13. Bae YH, Okano T, Hsu R, Kim SW (1987) Thermo-sensitive polymers as on-off switches for drug release. Macromol Rapid Commun 8:481–485
14. Cho DG, Sessler JL (2009) Modern reaction-based indicator systems. Chem Soc Rev 38:1647–1662
15. Basabe-Desmonts L, Reinhoudt DN, Crego-Calama M (2007) Design of fluorescent materials for chemical sensing. Chem Soc Rev 36:993–1017
16. Chaterji S, Kwon IK, Park K (2007) Smart polymeric gels: redefining the limits of biomedical devices. Prog Polym Sci 32:1083–1122
17. Tanaka T, Fillmore DJ (1979) Kinetics of swelling of gels. J Chem Phys 70:1214–1218
18. Kuckling D, Vo CD, Wohlrab SE (2002) Preparation of nanogels with temperature-responsive core and pH-responsive arms by photo-cross-linking. Langmuir 18:4263–4269

19. Kuckling D, Vo CD, Adler HJP, Volkel A, Colfen H (2006) Preparation and characterization of photo-cross-linked thermosensitive PNIPAAm. Macromolecules 39:1585–1591
20. Beines PW, Klosterkamp I, Menges B, Jonas U, Knoll W (2007) Responsive thin hydrogel layers from photo-cross-linkable poly(N-isopropylacrylamide) terpolymers. Langmuir 23:2231–2238
21. Pitois O, Francois B (1999) Crystallization of condensation droplets on a liquid surface. Colloid Polym Sci 277:574–578
22. Maruyama N, Koito T, Nishida J, Sawadaishi T, Cieren X, Ijiro K, Karthaus O, Shimomura M (1998) Mesoscopic patterns of molecular aggregates on solid substrates. Thin Solid Films 327–329:854–856
23. Yabu H, Shimomura M (2005) Simple fabrication of micro lens arrays. Langmuir 21:1709–1711
24. Tsuji S, Kawaguchi H (2005) Colored thin films prepared from hydrogel microspheres. Langmuir 21:8439–8442
25. Maeda Y, Yoshida R (2009) Fabrication of micropatterned thermosensitive gel with highly-ordered honeycomb surface and inverse opal structure. Biomed Microdevices 11:809–815
26. Engelman DM (2005) Membranes are more mosaic than fluid. Nature 438:578–580
27. Tanford C (1978) The hydrophobic effect and the organization of living matter. Science 200:1012–1018
28. Janda CY, Li J, Oubridge C, Hernandez H, Robinson CV, Nagai K (2010) Recognition of a signal peptide by the signal recognition particle. Nature 465:507–510
29. Kim BS, Basavaraja C, Jo EA, Kim DG, Huh DS (2010) Effect of amphiphilic copolymer containing ruthenium tris(bipyridyl) photosensitizer on the formation of honeycomb-patterned film. Polymer 51:3365–3371
30. Roncali J (1997) Linearly extended π-donors: when tetrathiafulvalene meets conjugated oligomers and polymers. J Mater Chem 7:2307–2321
31. Kim JK, Basavaraja C, Yamaguchi, Rabai G, Huh DS (2013) Reversible adsorption–desorption oscillations of nanoparticles on a patterned hydrogel surface induced by a pH oscillator in a closed chemical system. J Phys Chem B 70:207–220
32. Zhao ZX, Li Z, Xia QB, Bajalis E, Xi HX, Lin YS (2008) Swelling/deswelling kinetics of PNIPAAm hydrogels synthesized by microwave irradiation. Chem Eng J 142:263–270